Improved performance of CdS powder-based hybrid solar cells through surface modification

Yüzey modifikasyonu yardımıyla CdS toz bazlı hibrit güneş pillerinde performans artışı

Ahmet ÜNVERDİ[1,a], Salih YILMAZ*[2,b], Murat TOMAKİN[3,c], İsmail POLAT[4,d], Emin BACAKSIZ[5,e]

[1] Department of Physics, Faculty of Science, Istanbul University, Vezneciler, 34134, Istanbul, Turkey

[2] Department of Materials Science and Engineering, Faculty of Engineering, Adana Alparslan Türkeş Science and Technology University, 01250, Adana, Turkey

[3] Department of Physics, Faculty of Arts and Sciences, Recep Tayyip Erdogan University, Rize, Turkey

[4] Department of Energy Systems Engineering, Faculty of Technology, Karadeniz Technical University, Trabzon, Turkey

[5] Department of Physics, Faculty of Sciences, Karadeniz Technical University, 61080, Trabzon, Turkey

Abstract

The effects of surface modification of CdS through organic Eosin-Y, indoline D205, and Ru-based complex N719 and N3 dyes on CdS-based hybrid solar cells were studied. Chemical bath deposition (CBD) and doctor blade methods were in turn employed to fabricate the CdS specimens on Indium-Tin Oxide (ITO) covered glass substrates. P3HT material with and without dye coatings was covered through a spin-coater on the surface of CdS specimens. Ag paste was then deposited on the surface of P3HT to obtain hybrid solar cells. Structural analysis indicated that CdS powders showed a cubic growth with the preferred orientation of (111). Morphological analysis demonstrated that CdS powders exhibited hierarchical morphology and the morphology turned to granular structure with some porosity upon deposition of both N3 dye and P3HT layers. Absorption plots indicated that Eosin-Y dye loading led to a rise in the absorbance values of CdS specimens. After dye loading, photoluminescence data of CdS-based heterostructure illustrated a decrement in the luminescence intensity, implying that effective exciton dissociation was obtained. Current density-voltage (J-V) characteristics of the hybrid solar cells depicted that the best overall efficiency was observed for Eosin-Y-modified cell as 0.135%. This proved that surface modification by Eosin-Y dye led to a better interfacial contact between CdS and P3HT bilayer due to the enhancement in the charge separation.

Keywords: CBD, CdS powder, Hybrid solar cells, P3HT, Surface modification

Öz

CdS-tabanlı hibit güneş pillerinde, CdS'nin yüzey modifikasyon etkileri organik Eosin-Y, indolin D205 ve Ru bazlı N719 ve N3 boyaları vasıtasıyla incelendi. CdS örneklerini İndiyum-Kalay Oksit (ITO) kaplı cam altlıklar üzerinde büyütmek için, sırasıyla kimyasal banyo çökeltme (CBD) ve doktor bıçak yöntemleri kullanıldı. Boya kaplamaları olan ve olmayan CdS örneklerinin yüzeyine P3HT materyali, spin kaplama (spin-coater) cihazı yardımıyla kaplandı. Devamında Ag pasta, hibit güneş pillerini tamamlamak için P3HT yüzeyine çökeltildi. Yapısal analiz, CdS tozlarının kübik yapıda ve (111) tercihli yönelime sahip olduğunu gösterdi. Morfolojik analiz, CdS tozlarının hiyerarşik morfolojide olduğunu ve morfolojinin hem N3 boyası hem de P3HT tabakasının çökeltilmesiyle birlikte taneli ve gözenekli yapıya döndüğünü gösterdi. Soğurma (absorbsiyon) grafikleri, Eosin-Y boya kaplamasının CdS örneklerinin soğurma değerinde bir artışa yol açtığını gösterdi. Boya kaplamasının, CdS tabanlı heteroyapının fotolüminesans şiddetinde azalma oluşturması, etkin bir eksiton ayrışması elde edildiğini ortaya koymaktadır. Hibit güneş pillerinin akım yoğunluğu-voltaj (J-V) karakteristiklerinden, Eosin-Y modifikasyonlu güneş pilinin veriminin % 0,135 olarak en yüksek değerde olduğu tespit edildi. Bu durum, Eosin-Y boyası ile yapılan yüzey modifikasyonunun, yük ayrışmasında oluşturduğu iyileşmeden dolayı, CdS ve P3HT ikili yapısının arasında daha iyi bir ara yüzey teması sağladığını ispatlamaktadır.

Anahtar kelimeler: *CBD, CdS tozu, Hibrit güneş pilleri, P3HT, Yüzey modifikasyonu*

*b Salih YILMAZ; slh_yilmaz@yahoo.com.tr, Tel: (0322) 455 00 00 (2063), b orcid.org/0000-0002-3006-4473
a orcid.org/0000-0001-6144-1158   c orcid.org/0000-0003-1887-848X   d orcid.org/0000-0002-5134-0246
e orcid.org/0000-0002-0041-273X*

1. Introduction

A great interest has been gained on hybrid and organic solar cells for the use of photovoltaic applications over the last two decades due to their low charge mobility, simple deposition process and capacity for the low-cost electricity production as well as the continuous enhancement on their power conversion efficiency (PCE) values compared with the current inorganic semiconductor technology, based on energy with high-cost electricity production. As a result of combining by inorganic electron acceptor and organic electron donor layers, hybrid solar cells are formed. These solar cells merge flexibility of organic semiconductors with high electron mobility and excellent physical and chemical stability of inorganic-based ones (Cortina et al., Hu 2012; Kumar and Dutta, 2014). Various semiconductor nanoparticles such as CdSe (Greenham et al., 1997; Li et al., 2018), TiO$_2$ (Kang et al., 2018; Sun et al., 2014), PbS (Sonavane et al., 2018) and CdS (Kim et al., 2011; Yılmaz 2015) have been researched and among these, CdS nanostructures have demonstrated noticeable importance owing to their transport properties and high electron mobility (Yılmaz 2015). As an inorganic material, CdS is one of the most promising semiconductors due to its low resistivity, good photosensitivity, stability, moderate and direct band gap of 2.42 eV at room temperature (Xia et al., 2011). CdS powder can be produced through different methods such as electrostatic assisted aerosol jet deposition (EAAJD) method (Su et al., 2001), co-precipitation method (Liu et al., 2010), successive ionic layer adsorption and reaction (SILAR) (Ravichandran and Porkodi, 2018) and chemical bath deposition (CBD) technique (Yılmaz et al., 2019). Among these, CBD is a noncomplex method that provides low-cost production in a short time.

It is obvious that the impact of interfacial modification on the efficiency of hybrid solar cells is significant. Literature search shows that the population of reported studies on the surface or interfacial modification of CdS/P3HT hybrid solar cells is limited although there are plenty of works on ZnO (Ko et al., 2018; Pei et al., 2018; Tang et al., 2016) and TiO$_2$-based hybrid solar cells (Lin et al., 2009; Xia et al., 2013). In this work, CdS powders were precipitated using CBD route. The obtained CdS powder was then used to attain a CdS paste and afterwards, this paste was synthesized by the doctor blade method on ITO coated glass slides. After the CdS samples were fabricated by doctor blade method, four different dyes which are N719 and N3 (Ru-based complex dyes), Eosin-Y (organic dye) and D205 (indoline dye) were used as interfacial modification for CdS/P3HT heterostructures due to their improving character of the surface properties of CdS. A positive chance in the chemical and physical properties of the surface of CdS is expected to be seen by obtaining further photocurrent with these dyes (Zhong et al., 2014).

2. Experimental procedure

2.1. Fabrication of CdS thin films

CdS powders were fabricated through CBD route first. Commercial cadmium chloride (CdCl$_2$), thiourea (CH$_4$N$_2$S), ammonium chloride (NH$_4$Cl) salts, ammonium hydroxide (NH$_4$OH) (Sigma-Aldrich Co.) and deionized water were used to prepare the essential solution. In the production process of CdS powders, 80 ml of 0.20 M thiourea and 80 ml of 0.08 M CdCl$_2$ were used as S^{2-} and Cd^{2+} origins, respectively. 80 ml of 0.20 M NH$_4$Cl and 56 ml of NH$_4$OH were employed as a complexing agent and buffer, respectively. After all solutions dissolved separately in the beakers, they were poured and mixed in a beaker and 4 ml of deionized water was added to form the final stock solution. The beaker was put in an ultrasonic bath and kept there 3 minutes to make sure that all materials were dissolved. The pH rate of the mixed solution was appeared as 11. Then, the beaker was put on a hot plate and the temperature was slowly increased to 75 °C and kept there until the solution fully evaporates. After the evaporation of solution, the CdS powders were obtained.

Commercial ITO substrates (7.5x5 cm^2) were cut as 1.5x1.25 cm^2 and were in turn bathed ultrasonically dilute sulfuric acid, distilled water, and absolute ethyl alcohol as 10 minutes for each step and subsequently, the substrates were drained by flowing of dry nitrogen. Afterwards, the obtained CdS powders (0.4 g) were utilized to prepare a paste including 20 µl of acetyl acetone, 100 µl TX-100 and 8 ml deionized water. The prepared paste was stirred manually and constantly to get rid of bubbles. Then, the paste was deposited on ITO substrates by doctor blade method and the substrates were annealed at a temperature of 350 °C for 30 minutes on a hot plate to finalize CdS paste-based heterostructures.

2.2. Preparation of diverse dyes and surface modification

5 mM Eosin-Y and 0.3 mM D205 dye were dissolved in acetone and in a mixed solution of equimolar acetonitrile and tert-butyl alcohol,

respectively, while equimolar of 0.5 mM N719 and N3 dyes were dissolved in absolute ethyl alcohol. For each dye solution, CdS samples were immersed and kept there for 24 hours. After 24 hours, it was realized that the dye coatings on the surface of CdS thin films were deficient. Therefore, to overcome this issue, spin coating technique was utilized additionally for each dye to obtain well-coated dye on CdS specimens' surfaces. During spin coating process, the speed of rotation and the sum of repeats were set as 1000 rpm and 20 rounds; 1500 rpm and 15 rounds; 1000 rpm and 15 rounds; 1000 rpm and 10 rounds for Eosin-Y, D205, N3 and N719, respectively. Each coating step was applied for 1 min for each dye loading.

2.3. Production of CdS powder/P3HT hybrid solar cells

2 ml chlorobenzene was used as a solvent for 20 mg commercial P3HT material and the final solution was applied to each with and without dye-modified CdS-based heterostructures. This process was carried out by a spin-coater and the speed of rotation, sum of repeats and coating duration were set as 1000 rpm, 5 times and 1 minute, respectively. CdS/P3HT hybrid solar cells were finalized by employing Ag paste as back and front contacts with a contact area of 8×10^{-3} cm^2. The produced CdS samples (pristine, hybrid unmodified and surface modified through diverse dyes) were coded between D0–D5 after the fabrication processes were carried out and are stated in Table 1.

Table 1. Codes and names of the produced samples

Code	Sample
D0	ITO/CdS paste
D1	ITO/CdS paste/P3HT/Ag
D2	ITO/CdS paste/Eosin-Y/P3HT/Ag
D3	ITO/CdS paste/D205/P3HT/Ag
D4	ITO/CdS paste/N719/P3HT/Ag
D5	ITO/CdS paste/N3/P3HT/Ag

2.4. Characterization

The structural characterization of CdS specimens was carried out at room temperature by X-ray diffraction measurement (Rigaku SmartLab Unit) using CuKα radiation with a step of 0.01° in the interval of 20-60°. Scanning electron microscopy (SEM, JEOL JSM 6610) was employed for the surface morphology of fabricated samples where energy dispersive X-ray spectroscopy (EDS, Oxford Instruments) were used to analyze the elemental ingredients of the samples. To obtain absorption spectra measurements and optical

transmittance of specimens, UV-VIS spectrophotometer (SpectraMax M5) was employed in the wavelength between 400 and 1000 nm. To perform the photoluminescence (PL) analysis, Xenon flash lamb (Dongwoo Optron equipment) was employed at room temperature with a maximum capability of 450 W. PL measurements for CdS samples were carried out employing a 325 nm excitation wavelength, whereas a laser was used for the other samples with a 532 nm excitation wavelength. To measure the J (current density) – V (voltage) characteristics of produced CdS/P3HT hybrid solar cells, a source-meter (Keithley 2401) with a power output of 93 mW/cm^2 was employed under a solar simulator (AM 1.5).

3. Results and discussion

Fig. 1 indicates the XRD curve of CdS powder. Reflection planes (111), (200), (220) and (311) show that CdS specimens have polycrystalline architecture that is assigned to cubic zincblende phase (JCPDS card no: 75-1546). Except for cubic CdS peaks, there seem few peaks that might be related to the ITO substrate. Also, it is observed from the literature studies that CdS samples, which were grown by chemical bath deposition (CBD), generally crystallize in cubic structure (Khallaf et al., 2008). The preferred orientation is along the (111) reflection plane and is quite strong. Lattice constant, *a* is determined from (111) plane and it is found to be 0.581 nm. The crystallite size (D) is calculated by Scherrer equation (Patterson, 1939) and it is found to be 16.3 nm, meaning that CdS powders exhibit nanocrystalline structure.
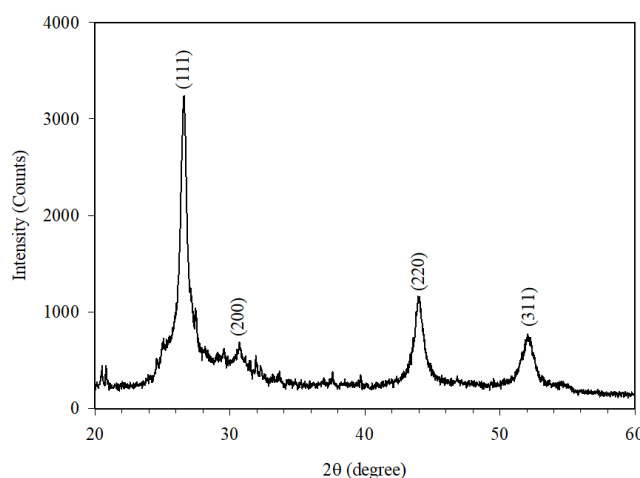
Figure 1. XRD curve of CdS powder

Fig. 2(a)-(c) show the SEM top view data of CdS powder, D1 and D4, respectively and Fig. 2(d) illustrates the cross-sectional view of D4. It is seen from Fig. 2(a) that CdS powders are formed in the hierarchical morphology with some voids. It is also appeared that CdS powders are composed of crystallites with a very small in size. Fig. 2(b) demonstrates that the voids in CdS powders are mostly filled by P3HT layer after the spin-coating of P3HT on the D0 structure while hierarchical morphology are almost preserved. Besides, a

diverse surface morphology is gathered for D4. Fig. 2(c) shows a porous and granular morphology for P3HT thin film. This can be explained by the smoother P3HT thin film coating that is possible by N719 dye modification which is homogenizing the surface of CdS paste. However, P3HT surface is appeared to be rough. It is seen from Fig. 2(d) that the thickness of D4 heterostructure is about 28 μm. High thickness value of the heterostructure is substantially due to the thickness of CdS paste. The other devices also showed similar thickness values.
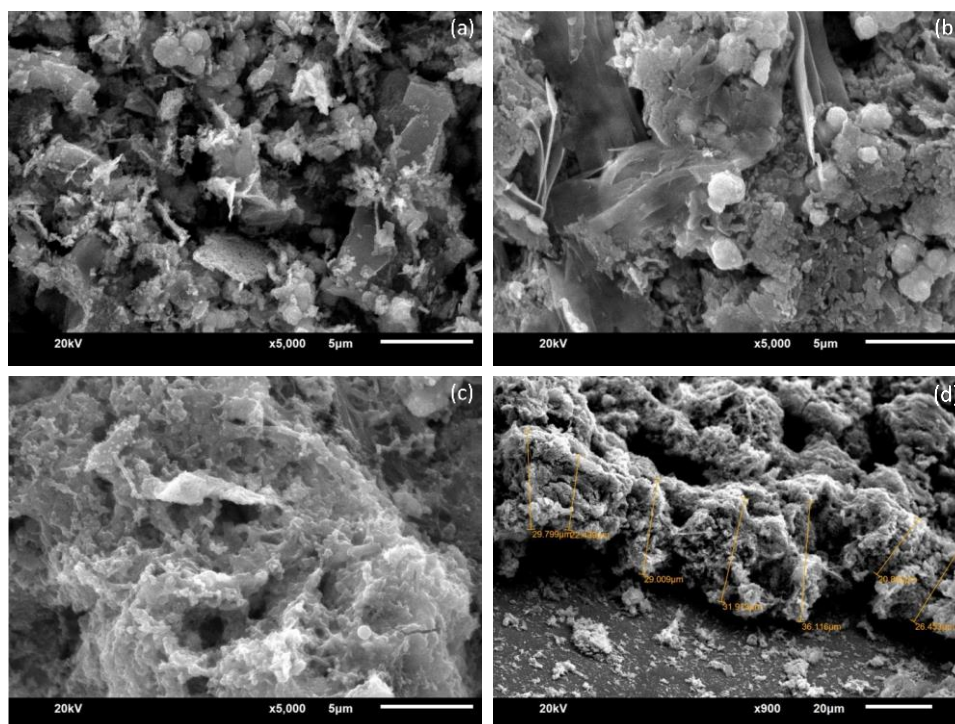
Figure 2. SEM top view data of (a) CdS powder, (b) D1, (c) D4 and (d) shows the cross-sectional view of (c)

Fig. 3 depicts EDS survey spectrum of CdS powder. It is remarkable that there is no other ingredient except for Cd and S atoms in the spectrum. Also, Cd/S molar ratio which is about 1.13 can be seen from the inset of the figure.

However, nonstoichiometric CdS sample is occurred as a result of the creation of sulfur vacancies (V_S) and cadmium interstitials (I_{Cd}) defects (Yılmaz et al., 2019).
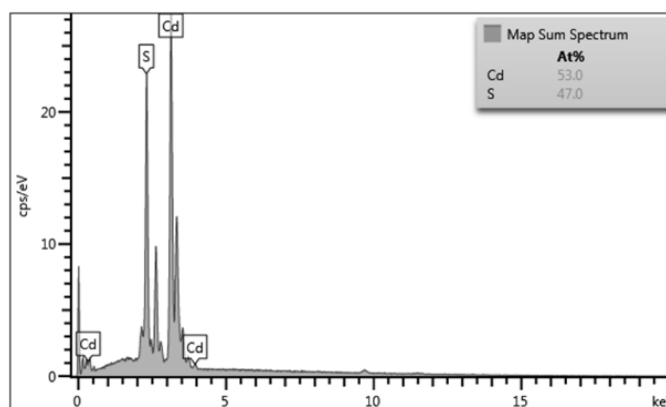
Figure 3. EDS survey spectrum of CdS powder

Fig. 4 indicates absorption curves of D1, D2, D3, D4 and D5 layers. It is realized that D1 layer shows a wide absorption in the wavelength interval between 300 and 650 nanometers, having the highest absorbance point for the wavelength of 615 nanometers that might be akin to the vibronic transition of P3HT material due to the intense chain interactions (Yılmaz et al., 2019). D2 shows a very similar characteristic to D1 except for its higher absorbance value through the curve. D3 structure exhibits an absorbance value between with and without Eosin-Y modified CdS/P3HT (D2 and D1) structures in the wavelength interval of 300-650 nm while it shows a lower value in the interval of 650-1000 nm. However, D4 structure shows the same characteristics although its peak value is the lowest whereas D5 structure has the same characteristics with D1 in terms of its intensity and shape. The reason for the decrease of D4 in the intensity and a narrowing in the absorption band could be attributed to the less compatible interface between CdS paste and P3HT and less photon harvesting, respectively. Thus, it can be declared that D2 heterostructure shows the highest absorbance intensity, proving the positive effect of surface modification via Eosin-Y dye on CdS sample's surface due to intense π-π interactions between P3HT polymer chains that leads to a rise in the spatial packing of P3HT as well as a better interface for D1 (Nan et al., 2013).
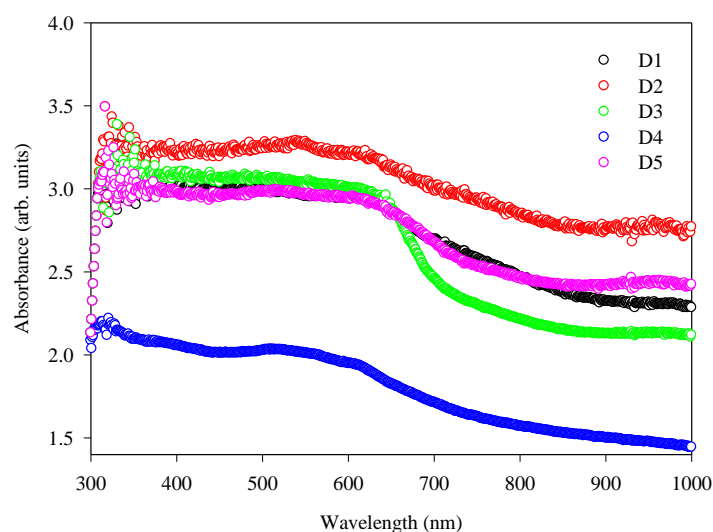
Figure 4. Absorption plots of D1, D2, D3, D4, D5

Fig. 5(a) and (b) illustrate the PL curves of CdS powder and D1, D2, D3, D4 and D5, respectively. The CdS powder sample exhibits three fundamental peaks corresponding to different regions that are 350-400 nm (UV), 400-500 nm (blue) and 500-750 nm (deep level emission), respectively and the strongest peak is seen at 570 nm. The root of this strong peak might be akin to the intrinsic defects that include I_{Cd}, I_S and V_S that is caused by nonstoichiometric growth of CdS powders, which is in good agreement with the EDS conclusion (Yılmaz et al., 2017). The UV peak is associated with transitions between shallow and deep levels, while the blue peak is attributed to defect levels (Yılmaz et al., 2015). On the other hand, deep level emission is generally attributed to internal defects such as I_{Cd}, V_S and V_{Cd} (Yılmaz et al., 2017). In Fig. 5(b), it is realized that D205 and Eosin-Y modified (D3 and D2) heterostructures show similar curve, but different peak intensities with nonmodified one whereas N719 and N3 (D4 and D5) modified heterostructures show both different curve shape and peak intensities at 716 nm. This means that P3HT film dominates all the spectra. Diverse dye modified CdS-based heterostructures exhibit lower PL intensities than those of CdS/P3HT (D1), showing that PL intensity diminishes via surface modification due to an active electron transfer between CdS and P3HT layers, which improves the efficient exciton separation at the interface of D1 bilayer (Yılmaz et al., 2019; Zhong et al., 2012). Hence, dye modification causes the creation of a better interface for D1, which is consistent with optical absorption results discussed previously. Analogue results were obtained by Jabeen et al. for CdS/P3HT hybrid solar cells (Jabeen et al., 2018).
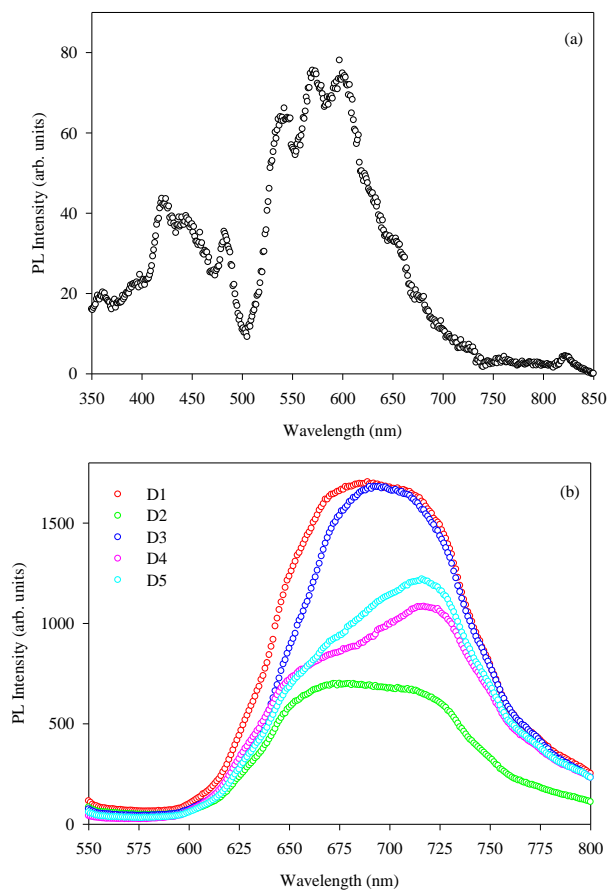
Figure 5. PL curve of (a) CdS powder and (b) PL data of D1, D2, D3, D4, D5

Fig. 6 and Table 2 represent J-V characteristics of D1, D2, D3, D4 and D5 hybrid solar cells and J_{sc}, V_{oc}, FF and (Ⅱ) parameters of CdS-based hybrid solar cells, respectively. It is observed that each cell showed a photovoltaic response. It is noticed that nonmodified (D1) hybrid solar cell displays a short circuit current density (J_{sc}) of 0.32 mA.cm^{-2}, open circuit voltage (V_{oc}) of 0.48 V, fill factor (FF) of 0.28 and power conversion efficiency (Ⅱ) of 0.046% which is low. This is caused by the hydrophilic surfaces of P3HT and CdS, which leads to a weak interfacial contact area (Zhong et al., 2012). Another case of having a low PCE score might be attributed to PL data of CdS sample that has a defected structure, which was represented in Fig. 5(a) (Chen et al., 2011). Yılmaz and co-workers reported a lower PCE value of 0.015% for spray-deposited CdS based devices (Yılmaz et al., 2019). Unlikely nonmodified (D1) one, Eosin-Y modified (D2) hybrid solar cells show an increased J_{sc} value of 1.21 mA.cm^{-2} while a lower V_{oc} value of 0.40 is observed, which contributes a great enhancement in PCE score almost 3 times, that is, 0.135%. The increase in the J_{sc} value can be associated with the deposition of Eosin-Y dye molecules on CdS that gives rise to a better light absorption, which is also proved in Fig. 4, and the decrease in surface defects of CdS via Eosin-Y absorption (Lim et al., 2012; Luo et al., 2016). On the other hand, Eosin-Y dye modification leads to a decrement in the leakage currents by direct contact between CdS and Ag metal (Lim et al., 2013). However, the PCE values are even worse than that of pristine (D1) one via surface modification of the other D205, N719 and N3 (D3, D4 and D5) dyes, which can be seen in Table 1. This is in agreement with the absorption spectra presented in Fig. 4. That is, dye modification of CdS surfaces by D205, N719 and N3 dyes leads to a reduction in absorption curves so that the surfaces of CdS pastes are less coated with such dyes.
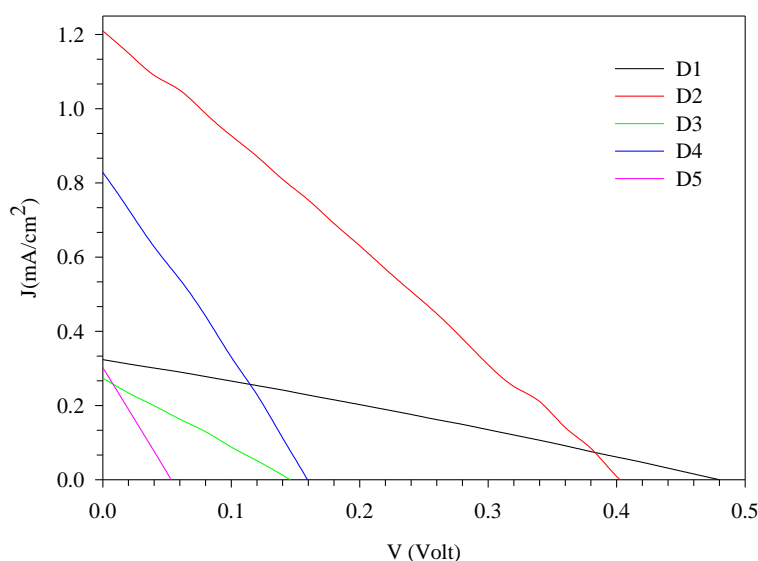
Figure 6. J-V characteristics of D1, D2, D3, D4 and D5

Table 2. J_{sc}, V_{oc}, FF and (Ƞ) parameters of CdS/P3HT hybrid solar cells

Cells	J_{sc} (mA.cm^{-2})	V_{oc} (V)	FF	Ƞ (%)
D1	0.32	0.48	0.280	0.046
D2	1.21	0.40	0.260	0.135
D3	0.27	0.14	0.265	0.011
D4	0.83	0.16	0.264	0.038
D5	0.30	0.05	0.267	0.004

4. Conclusions

CdS samples on ITO-coated glass substrates were produced by CDB and doctor blade methods. XRD data presented that CdS powders grew in the nanocrystalline structure. SEM conclusions showed that CdS powders exhibited hierarchical morphology whereas morphological structure became granular and porous by deposition of both N3 dye and P3HT layer. Absorbance plot indicated that CdS specimens modified via Eosin-Y (D2) dye showed the best absorption spectrum. Photoluminescence results displayed that CdS samples had a defected structure and the surface treatment via diverse dyes showed a decrement in the PL intensity, implying an enhancement in the ability of charge separation. J-V plot illustrated that in comparison with pristine (D1) one, a better result for PCE value, almost 3 times, was observed for D2 as 0.135%.

Acknowledgements

References

Chen, F., Qiu W., Chen, X., Yang, L., Jiang, X., Wang, M. and Chen, H. (2011). Large-scale fabrication of CdS nanorod arrays on transparent conductive substrates from aqueous solutions. Solar Energy, 85(9), 2122-2129. https://doi.org/10.1016/j.solener.2011.05.020.

Cortina, H., Pineda, E. and Hu, H. (2012). Measurement of charge carrier recombination rates in planar hybrid CdS/poly3-octylthiophene solar cells. Solar Energy, 86(4), 1004-1009. https://doi.org/10.1016/j.solener.2011.06.003.

Greenham, N. C., Peng, X. and Alivisatos, A. P. (1997). Charge separation and transport in conjugated polymer/cadmium selenide nanocrystal composites studied by photoluminescence quenching and photoconductivity. Synthetic Metals, 84(1–3), 545-546. https://doi.org/10.1016/s0379-6779(97)80852-1.

Jabeen, U., Adhikari, T., Pathak, D., Shah, S. M. and Nunzi, J. M. (2018). Structural, optical and photovoltaic properties of P3HT and Mn-doped CdS quantum dots based bulk heterojunction hybrid layers. Optical Materials, 78, 132-141. https://doi.org/10.1016/j.optmat.2018.02.019.

Kang, M., Kim, S. W. and Park, H. Y. (2018). Optical properties of TiO2 thin films with crystal structure. Journal of Physics and Chemistry of Solids, 123, 266-270. https://doi.org/10.1016/j.jpcs.2018.08.009.

Khallaf, H., Oladeji, I. O., Chai, G. and Chow, L. (2008). Characterization of CdS thin films grown by chemical bath deposition using four different cadmium sources. Thin Solid Films, 516(21), 7306-7312. https://doi.org/10.1016/j.tsf.2008.01.004.

Kim, J., Choi, H., Nahm, C., Moon, J., Kim, C., Nam, S., Jung, D. R. and Park, B. (2011). The effect of a blocking layer on the photovoltaic performance in CdS quantum-dot-sensitized solar cells. Journal of Power Sources, 196(23), 10526-10531. https://doi.org/10.1016/j.jpowsour.2011.08.052.

Ko, Y., Kim, Y., Kong, S. Y., Kunnana, S. C. and Jun, Y. (2018). Improved performance of sol–gel ZnO-based perovskite solar cells via TiCl4 interfacial modification. Solar Energy Materials and Solar Cells, 183, 157-163. https://doi.org/10.1016/j.solmat.2018.04.021.

Kumar, N. and Dutta, V. (2014). Fabrication of polymer/cadmium sulfide hybrid solar cells [P3HT:CdS and PCPDTBT:CdS] by spray deposition. Journal of Colloid and Interface Science, 434, 181-187. https://doi.org/10.1016/j.jcis.2014.07.047.

Li, C., Wang, F., Chen, Y., Wu, L., Zhang, J., Li, W., He, X., Li, B. and Feng, L. (2018). Characterization of sputtered CdSe thin films as the window layer for CdTe solar cells. Materials Science in Semiconductor Processing, 83, 89-95. https://doi.org/10.1016/j.mssp.2018.04.022.

Lim, E. L., Yap, C. C., Yahaya, M. and Salleh, M. M. (2012). ZnO nanorod arrays coated with Eosin-Y at different concentrations for inverted bulk heterojunction organic solar cells. Advanced Materials Research, 501, 214-218.

https://doi.org/10.4028/www.scientific.net/AMR.501.214.

Lim, E. L., Yap, C. C., Yahaya, M. and Salleh, M. M. (2013). Enhancement of ZnO nanorod arrays-based inverted type hybrid organic solar cell using spin-coated Eosin-Y. Semiconductor Science and Technology, 28, 045009-045015. https://doi.org/10.1088/0268-1242/28/4/045009.

Lin, Y. Y., Chu, T. H., Li, S. S., Chuang, C. H., Chang, C. H., Su, W. F., Chang, C. P., Chu, M. W. and Chen, C. W. (2009). Interfacial nanostructuring on the performance of polymer/TiO2 nanorod bulk heterojunction solar cells. Journal of the American Chemical Society, 131, 3644-3649. https://doi.org/10.1021/ja8079143.

Liu, H., Zhang, K., Jing, D., Liu, G. and Guo, L. (2010). SrS/CdS composite powder as a novel photocatalyst for hydrogen production under visible light irradiation. International Journal of Hydrogen Energy, 35(13), 7080-7086. https://doi.org/10.1016/j.ijhydene.2010.01.028.

Luo, S., Shen, H., Zhang, Y., Li, J., Oron, D. and Lin, H. (2016). Inhibition of charge transfer and recombination processes in CdS/N719 co-sensitized solar cell with high conversion efficiency. Electrochimica Acta, 191, 16-22. https://doi.org/10.1016/j.electacta.2016.01.055.

Nan, Y. X., Li, J. J., Fu, W. F., Qiu, W. M., Zuo, L. J., Pan, H. B., Yan, Q. X., Chen, X. G. and Chen, H. Z. (2013). Performance enhancement of CdS nanorod arrays/P3HT hybrid solar cells via N719 dye interface modification. Chinese Journal of Polymer Science, 31(6), 879-884. https://doi.org/10.1007/s10118-013-1274-z.

Patterson, A.L. (1939). The Scherrer formula for X-ray particle size determination. Physical Reviews, 56 (10), 978. https://doi.org/10.1103/PhysRev.56.978.

Pei, J., Feng, K., Wei, Y., Zhao, X., Hao, Y., Li, Y., Sun, B., Chen, S. and Lv, H. (2018). Influence of organic interface modification layer on the photoelectric properties of ZnO-based hybrid solar cell. Journal of Photochemistry and Photobiology A, Chemistry, 364, 551-557. https://doi.org/10.1016/j.jphotochem.2018.06.042.

Ravichandran, K. and Porkodi, S. (2018). Addressing the issue of under-utilization of precursor material in SILAR process: Simultaneous preparation of CdS in two different forms – Thin film and powder. Materials Science in Semiconductor Processing, 81, 30-37. https://doi.org/10.1016/j.mssp.2018.02.037.

Sonavane, D. K., Jare, S. K., Kathare, R. V., Bulakhe, R. N. and Shim, J. J. (2018). Chemical synthesis

of PbS thin films and its physicochemical properties. Materialtoday: Proceedings, 5(2–2), 7743-7747. https://doi.org/10.1016/j.matpr.2017.11.451.

Su, B., Wei, M. and Choy, K. L. (2001). Microstructure of nanocrystalline CdS powders and thin films by Electrostatic Assisted Aerosol Jet Decomposition/Deposition method. Materials Letters, 47(1–2), 83-88. https://doi.org/10.1016/S0167-577X(00)00216-0.

Sun, W., Sun, K., Peng, T. Y., You, S., Liu, H., Liang, L., Guo, S. and Zhao, X. Z. (2014). Constructing hierarchical fastener-like spheres from anatase TiO2 nanosheets with exposed {001} facets for high-performance dye-sensitized solar cells. Journal of Power Sources, 262, 86-92. https://doi.org/10.1016/j.jpowsour.2014.03.086.

Tang, S., Tang, N., Meng, X., Huang, S. and Hao, Y. (2016). Enhanced power efficiency of ZnO based organic/inorganic solar cells by surface modification. Physica E: Low-dimensional Systems and Nanostructures, 83, 398-404. https://doi.org/10.1016/j.physe.2016.03.031.

Xia, C., Wang, N. and Kim, X. (2011). Mesoporous CdS spheres for high-performance hybrid solar cells. Electrochimica Acta, 56(25), 9504-9507. https://doi.org/10.1016/j.electacta.2011.08.047.

Xia, H., Zhanga, T., Wang, D., Wang, J. and Liang, K. (2013). Composite interfacial modification in TiO2 nanorod array/poly(3-hexylthiophene) hybrid photovoltaic devices. Journal of Alloys and Compounds, 575, 218-222. https://doi.org/10.1016/j.jallcom.2013.04.006.

Yılmaz, S. (2015). The investigation of spray pyrolysis grown CdS thin films doped with flourine atoms. Applied Surface Science, 357(A), 873-879. https://doi.org/10.1016/j.apsusc.2015.09.098.

Yılmaz, S., Atasoy, Y., Tomakin, M. and Bacaksız, E. (2015). Comparative studies of CdS, CdS:Al, CdS:Na and CdS:(Al–Na) thin films prepared by spray pyrolysis. Superlattices and Microstructures, 88, 299-307. https://doi.org/10.1016/j.spmi.2015.09.021.

Yılmaz, S., Polat, İ., Tomakin, M., Ünverdi, A. and Bacaksız, E. (2019). Enhanced efficiency of CdS/P3HT hybrid solar cell via interfacial modification. Turkish Journal of Physics, 43(1), 116-125. https://doi.org/10.3906/fiz-1810-21.

Yılmaz, S., Töreli, S. B., Polat, İ., Olgar, M. A., Tomakin, M. and Bacaksız, E. (2017). Enhancement in the optical and electrical properties of CdS thin films through Ga and K co-doping. Materials Science in Semiconductor

Processing, 60, 45-52. https://doi.org/10.1016/j.mssp.2016.12.016.

Yılmaz, S., Ünverdi, A., Tomakin, M., Polat, İ. and Bacaksız, E. (2019). Surface modification of CBD-grown CdS thin films for hybrid solar cell applications. Optik, 185, 256-263. https://doi.org/10.1016/j.ijleo.2019.03.156.

Zhong, M., Yang, D., Zhang, J., Shi, J., Wang, X. and Li, C. (2012). Improving the performance of CdS/P3HT hybrid inverted solar cells by interfacial modification. Solar Energy Materials and Solar Cells, 96, 160-165. https://doi.org/10.1016/j.solmat.2011.09.041.

Zhong, P., Que, W. X., Zhang, J., Yuan, Y., Liao, Y. L., Yin, X. T., Kong, L. B. and Hu, X. (2014). Enhancing the performance of poly(3-hexylthiophene)/ZnO nanorod arrays based hybrid solar cells through incorporation of a third component. Science China Physics, Mechanics & Astronomy, 57(7), 1289-1298. https://doi.org/10.1007/s11433-013-5213-3.